

A study of the quasi-static and low-velocity impact behavior of laminated CFRP composites

Mazin Y. Abbood¹, Simon Gill², Ahmed N. Uwayed¹,
Ahmed Mothanna³, Mohammed Ali⁴, Emad Kadum Njim*⁵,
Mujtaba A. Flayyih⁶ and Royal Madan

¹Dept. of Mechanical Engineering, College of Engineering, University of Anbar, Ramadi, Iraq

²School of Engineering, University of Leicester, University Road, Leicester, LE1 7RH, UK

³College of Engineering, University of Anbar, Ramadi, Anbar, Iraq

⁴Department of Medical Instruments Engineering Techniques, College of Engineering,
University of Al Maarif, Al Anbar, 31001, Iraq

⁵Ministry of Industry and Minerals, State Company for Rubber and Tires Industries, Iraq

⁶Prosthetics and Orthotics Engineering Department, College of Engineering,
AL-Mustaqbal University, 51001 Hillah, Babil, Iraq

⁷Department of Mechanical Engineering, Graphic Era (Deemed to be University),
Dehradun 248002, Uttarakhand, India

(Received June 9, 2025, Revised August 6, 2025, Accepted August 7, 2025)

Abstract. The applications of composite materials have been increasing significantly in recent decades due to their superior mechanical properties and versatility. The major effect limiting the use of composite materials is the lack of understanding of their response and their structural integrity under dynamic loads. Among the prominent damage mechanisms, the debonding under dynamic loading is a well-recognized failure mode for laminated composites. Up to date, the impact of the significant parameters on the delamination is thoroughly examined in this study with primary focus on the hemispheric indenter diameter and the characteristics of the exerted load applied at constant energy levels. The damage morphology has been carefully investigated using X-ray computed tomography, quantifying the shape and size variation of delamination areas across plies. The experimental observations have been incorporated into the finite element modeling, carried out in ABAQUS, by means of cohesive elements, which allow for the setting of a failure criterion. The main delamination area has been confirmed to be localized on the tension side of the laminate, where the most bending stress is sustained. Moreover, the angular difference between adjacent plies that articulates the distribution of the interlaminar stresses has to be taken into consideration, since it has a great impact on the extent of delamination. It is concluded that the initiation of delamination can be detected using a delamination threshold load based on the quasi-static load-displacement curve. These results illustrate the importance of the indenter radius to thickness ratio as a governing parameter in the structural response of composite plates, aiding in the development of more accurate predictive models for damage assessment.

Keywords: CFRP laminates; composite; delamination; quasi-static impact and cohesive zone model

*Corresponding author, Professor, Ph.D., E-mail: emad.njim@gmail.com

Copyright © 2025 Techno-Press, Ltd.

http://www.techno-press.org/?journal=acd&subpage=7

ISSN: 2383-8477 (Print), 2466-0523 (Online)

1. Introduction

Advanced composite materials, alongside Aluminium alloys and titanium alloys, have been progressively developed as next-generation materials for high-performance structural applications since the 1970s (Vini and Daneshmand 2022). Such materials are preferred in several industries, including aerospace, automotive, and marine, due to their remarkable characteristics, which include high specific strength, high modulus, excellent fatigue performance, corrosion resistance, and low thermal conductivity. These properties allow wider usage for tough environments that lead to improved structural efficiency and durability (Akbulut *et al.* 2020, Narwariya *et al.* 2018, Polatov *et al.* 2020, Sindu *et al.* 2018). A large amount of work has been done to characterize and model the mechanical response of these materials, as well as to develop advanced tools to predict their damage tolerance in various applications (Ali and Hasan 2022, Ibrahim *et al.* 2021). Significantly, in new aircrafts like the Airbus A350 and Boeing B787, composite materials account for more than 50% of the structural weight, emphasizing their important role towards light and strong structures (Nguyen and Waas 2020).

Numerous studies have been performed to explain the delamination mechanisms and their contributions to the performance of composite laminates (Davies and Zhang 1995, Nolan 2012, Zhang 1998). It is known that there exists a damage threshold load (DTL) for composite laminates, where the DTL indicates a significant increase in the delamination propagation and a significant reduction in the strength of the composite laminate surrounding the delaminated area (Olsson *et al.* 2006, Schoeppner and Abrate 2000, Zhang *et al.* 2012). This phenomenon is identified by the force-displacement curve, which shows a significant slope change, referred to as the knee point load, this is the point at which structural compliance increases with subsequent damage progression. However, the complex behaviour of failure modes in composite laminates still represents a major challenge for the Aerospace sector for reliable damage resistance and tolerance assessments. These complexities require developing predictive models and experimental strategies that can be used to validate and control for the durability of composite-based structures under different loading regimes. Some authors tried to detect delamination within the composite plies through vibration-based damage detection techniques (Uwayed and Abbood 2022). Since DTL is a new concept that has been used to improve the design concept of composite laminates. The effect of incoming damage on composite laminates under quasi-static loading and low-velocity impact loading needs to be further explored. This kind of research is a key to enhancing predictive models and techniques used for evaluating the structural integrity and damage tolerance of composites. Other related studies written by (Mouthanna *et al.* 2018, Daneshmand *et al.* 2023, Kadum Njim *et al.* 2024, Hassan *et al.* 2025) on advanced materials included the investigation of the nonlinear vibration characteristics of imperfect functionally graded cylindrical panels with different types of stiffener configurations, mechanical, tribological, and electrical properties of laminated Al/SiC/Ni composites, and wear behavior of imperfect functionally graded components. Therefore, these analytically based investigations serve as a useful basis to understand the complex behaviour of materials, thereby paving the way for further DTL-related studies in composite laminates. In (Fayyadh 2021), the accuracy of ACI 440.2 code equations in predicting flexural and shear capacities of CFRP-repaired RC beams was examined by analyzing steel ratios and shear stirrup presence. The study proposes modified models that significantly improve prediction accuracy, reducing errors from 21-64% to within 2–7.3% across tested parameters. Further, (Panigrahi and Das 2016), demonstrate that foam-filled corrugated sandwich plates, especially with metallic foams, offer superior ballistic resistance compared to solid or unfilled structures. Finite element

analysis confirms their effectiveness, making them suitable alternatives for lightweight protective applications. Analyzed modular linkage-based deployable structures, highlighting efficient reconfigurability through crank-slider mechanisms and low-energy actuation methods (Phocas *et al.* 2022). According to (Başoğlu *et al.*, 2023), laminated carbon-fiber reinforced polymers (CFRPs) have garnered substantial attention in industries like aerospace, automotive, and defense because of their excellent strength-to-weight ratio and superior mechanical properties. Despite these benefits, CFRP laminates are susceptible to damage from low-velocity impacts and quasi-static loading, with delamination and matrix failure being the predominant concerns. Considerable recent studies have shown that quasi-static indentation examinations can reliably simulate the mechanical response characteristic of low-velocity impacts. For illustration, (Wang *et al.* 2023) utilized LS-DYNA-based simulations in conjunction with the Tsai–Wu failure criterion to investigate the progression of damage in thick composite laminates. (Xiao *et al.* 2023) dissected an innovative biomimetic laminated design and found an improvement in impact damage resistance and post-impact strength retention compared to conventional configurations. (Lin *et al.* 2023) developed a hybrid numerical model integrating Hashin failure theory with cohesive surface interactions to accurately predict delamination in auxetic CFRP laminates, achieving results that closely matched experimental data. Similarly, (Lan *et al.* 2023) analyzed how tensile preloading affects delamination under impact, demonstrating that prestress conditions have a significant effect on interlaminar failure mechanisms. Additionally, (Tie *et al.* 2020) introduced a surrogate-based optimization model for designing external patches on damaged carbon fiber reinforced polymer (CFRP) laminates to enhance impact resistance.

This work is essential for engineering applications that involve composite structures, especially those under possible impact loads. The importance of this work is to identify the damage within the back layers in the bending side away from the impact side to avoid catastrophic damage. Furthermore, using X-ray computed tomography to identify the shape of delamination plays a vital role in reducing this type of failure by choosing the best stack sequence.

This work aims to study the onset and growth of delamination under quasi-static and low-velocity loading conditions by studying the contact behavior of composite laminates. This research investigates the differences between quasi-static and low-velocity impact damage at similar energy levels and how each energy type affects the size and topology of delaminated areas between neighboring plies with different fiber orientations of interest (0/45, 45/90, 90/-45, and 45/-45). Furthermore, the effect of the indenter radius to plate thickness ratio on the applied force and damage evolution has been numerically studied over a wide range of plate thicknesses. The ratio of the spherical impactor's radius to the laminate's thickness is expected to control how the stress is distributed near the contact point. Hence, an important goal of this investigation is to assess the size effect of the impactor in cases where the dimensions of the impactor are on the same order of magnitude as the laminate thickness, and thus to gain significant information about the mechanics of damage initiation and propagation.

In engineering applications, the finite element method (FEM) is widely known as an effective method for modeling and solving mathematical equations. Over the last few decades, FEM has been employed extensively to address a variety of problems across many disciplines (Madanet *et al.* 2025, Uwayed *et al.* 2023). Due to the complex governing equations involved and the high number of variables that need to be taken into account, the method can be computationally intensive, despite its robustness and versatility. Several commercial software packages have been developed to address these challenges, including ANSYS and ABAQUS. A number of these tools can be used to improve computational efficiency and accuracy, thereby

shortening the time it takes to obtain reliable solutions to complex mathematical models (Abbas *et al.* 2025, Azeez Neamah *et al.* 2025, Khudhur *et al.* 2025, Alhous *et al.* 2025). The Finite Element Method (FEM) is used to define the delamination area between two consecutive plies using the commercial software package ABAQUS. Three-dimensional reconstructions using VG Studio software validate the numerical predictions against experimental observations from micro-computed tomography (micro-CT) scanning. In addition, to detect the real damage in a trapezoidal beam made of unidirectional carbon fiber reinforced polymer (CFRP), the Improved Curvature Damage Factor (ICDF_j) is used, which was proposed in (Brethee *et al.* 2023, Marir and Uwayed 2024). This integrated strategy, which merges high-fidelity numerical simulation methods with powerful experimental facilities, is intended to accelerate the understanding of the complex mechanisms that can lead to delamination and to assist in the design of more robust composite systems for demanding applications.

2. Multiscale computational analysis of composite materials

One of the key advantages of composite materials is that they can have tailored properties for a certain application, offering the possibility to control their macroscopic properties at a fine scale through their microscopic building blocks. Thus, the study of damage mechanisms in composite materials demands a multi-scale perspective, involving the phenomena at different levels: micro, meso, and macro, as shown in Fig. 1 (Olsson *et al.* 2006). This multi-scale approach aims to make links between the structural responses at the different scales through simplified but effective micro-models (LLorca *et al.* 2013). Within the multi-scale material modeling framework presented, properties at each scale are predicted and correlated using continuum mechanics principles. Three main strategies are used to simulate damage in composite structures: micro damage mechanics (MIDM), which concentrates on damage initiation and evolution at the constituent scales, mesoscopic damage mechanics, which analyzes ply-level interfacial interactions and inter-laminar failures, and macro damage mechanics (MADM), which assesses global failure modes and the overall structural integrity. The adoption of this framework provides a thorough insight into how damage evolves for the variety of time scales considered, thus allowing the design of composite structures with superior performance and increased durability for specific applications.

3. Cohesive-zone models

Delamination is a common type of damage in composite structures that significantly reduces the stiffness of the structure, especially under impact loading. The purpose of the damage modeling demands the simulation of the initiation and propagation phases of delamination (Johnson and Holzzapfel 2006, Tabiei and Zhang 2018). To represent the initiation phase, strength-based criteria are commonly used within the finite element (FE) methods (Zhou *et al.* 2020). The propagation stage is motivated by the J-integral-detached, the virtual crack extension, and VCCT methods that are used based on fracture mechanics (Kobayashi *et al.* 1973). This allows for the prediction of growth characterisation and propagation in molecular modelling of delamination behaviour, giving a clear idea calculation output of the degradation in the integrity of composite materials. Current modelling approaches have many limitations, including the inadequate

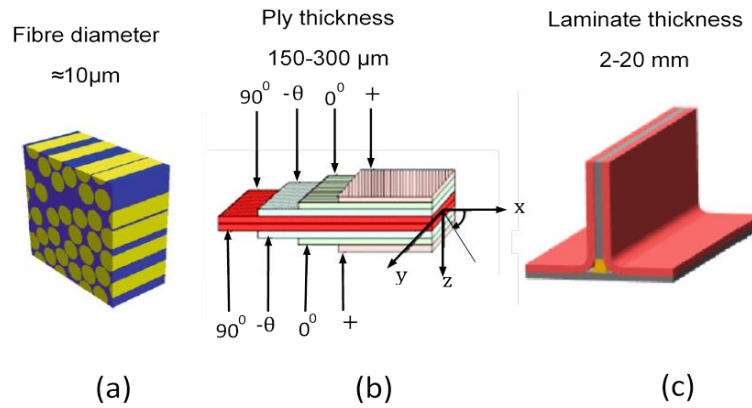


Fig. 1 Hierarchical representation of composite materials across different length scales: (a) microscopic level showing individual fibers and matrix, (b) mesoscopic level illustrating plies and laminate arrangement, and (c) macroscopic level representing the full structural component. Adapted from (Uwayed and Abbood 2022)

evaluation of material nonlinearity, therefore, the accuracy of damage prediction is often impaired. Further, these models often demand accurate input of a predetermined crack position, and due to the need for a very fine mesh, the simulation is computationally expensive and prevents the broad application of the method. In finite element analysis, the strength and toughness associated with intralaminar damage must be accurately represented to effectively simulate interlaminar damage in composite structures (Falzon and Apruzzese 2011, Liu and Zheng 2010). The need for these capabilities stems from the desire to realistically simulate the complex failure modes (delamination) exhibited by composite materials when subjected to various load conditions, enabling the generation of effective predictive tools to optimise composite design. Since nonlinearities are prevalent in both the material and geometric nature of the interface of stacked plies, a cohesive element technique has been used to model such behavior. The underlying idea is based on the thickness cohesive-zone model introduced in (Wimmer *et al.* 2009), which assumes that a plastic zone develops in front of the crack tips when the stresses in the material exceed the yield strength. The molecular forces acting at the same time as the glue provide a first concept of cohesive forces (Perillo and Jørgensen 2016), a more complex approach introduced by Barenblatt towards solving static problems in elastic bodies containing cracks. The cohesive element method allows accurate modeling of delamination onset and propagation by implementing these rules, offering valuable insights into the failure phenomena of composite systems. In this study, the properties of the cohesive material are illustrated in Table 1.

To investigate the evolution of stresses inside an elastic composite laminate, a simply supported composite laminate with $[0, 45, 90, -45]_s$ layup and $30 \times 30 \times 1 \text{ mm}^3$ dimensions has been simulated with properties illustrated in Table 2 under a rigid impactor, a steel impactor has been used. Generally, the impactor is 20 times stiffer than typical carbon epoxy. Thus, it can be modelled as a rigid body such that the deformations within the impactor are neglected (Nezhad *et al.* 2014). Modelling the impactor in this way will save computational time. In this study, the impactor was given a 1mm downward displacement. In this study, three different sizes of hemispherical impactors, 1, 2, and 4 mm in diameter, have been used with a mass of 350 g. 484 linear quadrilateral elements of type R3D4 have been used to mesh the impactor. The contact between

Table 1 Properties of interface material

| Properties | Symbol | Units | Value [Song, K., C.G. Dávila and C.A. Rose] |
|----------------------------------|--------|--------------------|--|
| Nominal stress mode I | tn | MPa | 60 |
| Nominal stress mode II | ts | MPa | 90 |
| Nominal stress mode III | tt | MPa | 90 |
| Elastic modulus normal direction | Knn | GPa | 1.2X10e3 |
| Elastic shear modulus | Kss | GPa | 1.2X10e3 |
| Elastic shear modulus | Ktt | GPa | 1.2X10e3 |
| Fracture toughness I | GI | N/m | 250 |
| Fracture toughness II | GII | N/m | 635 |
| Fracture toughness III | GIII | N/m | 732 |
| Density [Assumed] | ρ | Kg/mm ³ | 1.6e-9 |

Table 2 Mechanical properties of UD/M55J composite laminate

| Properties | Symbol | Units | Value [Song, K., C.G. Dávila and C.A. Rose] |
|-------------------------------|------------|-------|--|
| Young's Modulus 0° | E1 | GPa | 300 |
| Young's Modulus 90° | E2 | GPa | 12 |
| In-plane Shear Modulus | G12 | GPa | 3.6 |
| Major Poisson's Ratio | ν_{12} | | 0.30 |
| Ult. Tensile Strength 0° | Xt | MPa | 2738 |
| Ult. Comp. Strength 0° | Xc | MPa | 1459 |
| Ult. Tensile Strength 90° | Yt | MPa | 50 |
| Ult. Comp. Strength 90° | Yc | MPa | 250 |
| Ult. In-plane Shear Strength. | S | MPa | 96 |
| Density | | g/cc | 1.65 |

the hemispherical nose of the impactor and the top face of the CFRP must be modelled. This contact has been implemented using a surface-to-surface kinematic contact algorithm with finite sliding that is available in Abaqus 14.

4. Experimental procedure

Using two different sets of specimens, the present study aims to provide a detailed overview of the composite behavior (Raad *et al.* 2024, Mohammad *et al.* 2024). These consist of rectangular laminates, specifically 30 mm wide by 60 mm long by 1 mm thick. These laminates are made out of unidirectional (UD) carbon/epoxy prepreg based on the Cyte/configure/MTM44-1 resin and reinforced with M55J high-modulus carbon fibers. This material was provided by Multimatic CF Tech, a leading supplier of advanced composite materials. Table 2 systematically captures the mechanical properties of this composite system, which are essential for evaluating its performance under different loading conditions. These properties include important parameters like tensile



Fig. 2 Setup of the instrumented facility used for quasi-static testing

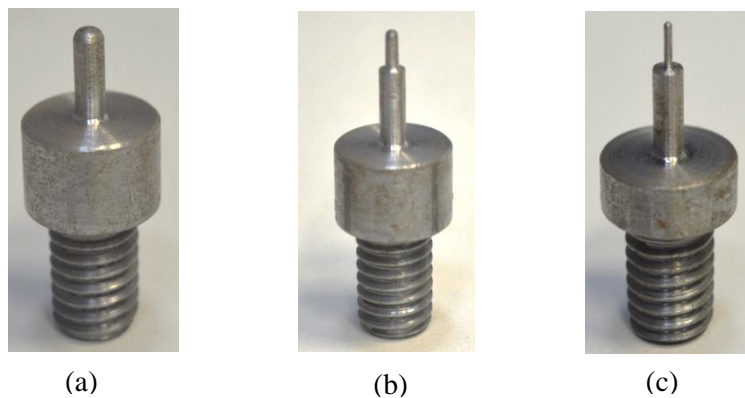


Fig. 3 Three indenters with varying diameters: (a) 4 mm, (b) 2 mm, and (c) 1 mm

strength, modulus of elasticity, and interlaminar shear strength, serving as critical metrics for assessing the material's structural integrity and damage tolerance in demanding applications.

4.1 Quasi-static testing

The quasi-static test experimental setup is indicated in Fig. 2, presenting the instrumented test facility used in this work. To perform indentation tests, a Hounsfield 10 kN universal testing machine was used, in which indenters were fixed into the lower jaw of the machine in such a way that forces were applied to the lower surface of the samples with a displacement speed of 1 mm/min. In order to ensure testing conditions were consistent for each specimen and minimize variation in the experimental results, all indenters experienced a constant total displacement of 1 mm. During the testing process, with the assistance of the in-house data acquisition system of the Hounsfield 10 kN universal testing machine, the applied force and the respective deflection at the back-face contact point of the laminate were monitored throughout. Across these ranges, the accuracy was high (i.e., $\pm 0.5\%$ of indicated values), and system precision is defined as the

repeatability of force and extension measurements under set displacement control. All the specimens were mounted on a circular support with an internal diameter of 25 mm, so they could rest freely during testing. The deflection on the laminate's back face's center was effectively measured using a centrally located sensor within the support, mitigating errors associated with indentation due to the upper surface of the laminate being penetrated by the steel indenter. The effect of indenter geometry was examined using three 1 mm, 2 mm, and 4 mm hemispherical head diameter rigid steel indenters, as shown in Fig. 3. The difference in indenter dimensions facilitated a systematic investigation of the influence of indenter size on the contact response and the damage progression in the composite laminates, which improved the understanding of the material behavior under local quasi-static loading.

5. Results and discussions

The quasi-static response of laminated carbon fiber reinforced polymer (CFRP) composites has been comprehensively investigated experimentally and numerically. Analytical predictions are systematically compared against experimental results in terms of relevant parameters, e.g., force-time and displacement-time curves, and the quantification of delaminated regions. Comparing numerical results with experimental data confirms that the models accurately capture the mechanical response and damage progression observed in the experiments, thus validating the numerical simulation approach and gaining insight into the behavior of CFRP laminates under a quasi-static load. More specifically, the focus is on clarifying how different indenters' diameters alter the response of the material, while describing the different nature of the early stages of the damage propagation. The data presented here is organized sequentially: experimental data is reported first, followed by data from numerical modeling, and concluding with a comparison of the two in a discussion subsection.

In an experimental setting, the quasi-static response of CFRP laminates is precisely defined in terms of the real-time recording of applied force and the respective displacement, as well as an in-depth characterization of the delamination process. The delamination area is calculated from finite element (FE) simulations including a cohesive layer model, which gives a good description of the initiation and propagation of interfacial damage. This comparative analysis not only highlights the experimental fidelity of the cohesive layer model but also reveals the differences between the simulated results and experimental results brought by varying the indenter diameters. This combined experimental-numerical methodology provides fundamental insights into the underlying damage mechanisms of CFRP laminates for quasi-static loading and thus improved performance of predictive models for advanced composite design and optimization.

5.1 Force-displacement behavior

Three different indenter diameters (1 mm, 2 mm, and 4 mm) underwent uniform displacement of 1 mm across the laminates. The applied displacement was incremented at a rate of 1 mm/min, which was considered slow enough to accurately represent quasi-static loading, since the kinetic energy yielded during the process is negligible with respect to the total energy or work done. The role of indenter diameter on the force-displacement response is well established, and the resulting force-displacement curves are analyzed to clarify the variations in mechanical response and damage progression as a function of indenter size.

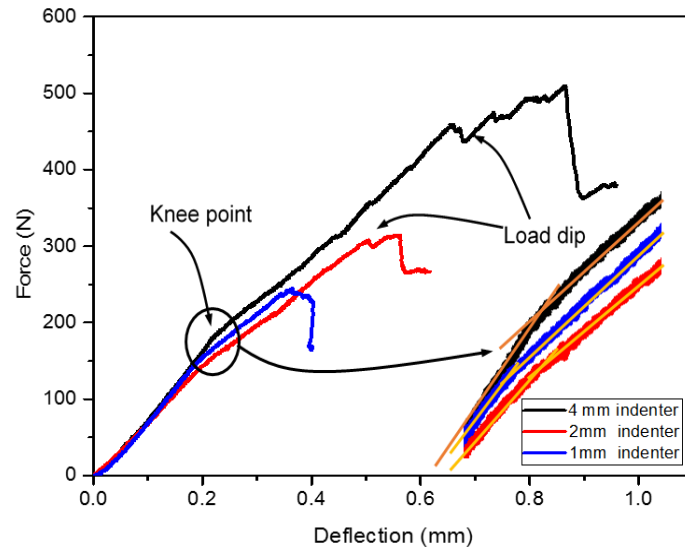


Fig. 4 Measured force-displacement curves corresponding to indenters with diameters of 1 mm, 2 mm, and 4 mm

The four phenomena described below about the force-displacement curves shown in Figure 4 are associated with the quasi-static behavior of laminated composites as a function of the indenter diameter (1 mm, 2 mm, and 4 mm) and yield important information about the mechanical response and damage development for the material.

(a) Elastic Region: The early part of the force-displacement curve exhibits an elastic deformation and is independent of indenter size. The slope in this area is the elastic stiffness of the laminate, which indicates resistance against deformation until the damage begins.

(b) Knee Point: A distinct transition, termed the knee point, is observed in the force-displacement curve at approximately 0.2 mm of displacement, where a significant change in the curve's slope is evident. This transition correlates with the onset of damage, mainly by delamination, and is characterized by reduced stiffness of the laminate. It is worth noting that while the total load at which the knee occurs varies with the indenter size, the slope thereafter remains relatively consistent across the three indenter sizes, highlighting that this feature is dominated more by the bending deformation as opposed to localized stresses imparted by the indenter being in contact with the sample. The knee point load does vary slightly with indenter size, the 1 mm indenter giving the lowest value, the 4 mm indenter the highest value, which is consistent with expectations of contact-related failure mechanisms. This suggests that the size of indenters has a minor effect on the initiation of delamination. A sharp decline in laminate stiffness due to delamination, which is observable for a 2 mm indenter, also contributed to the loss in slope after the knee point.

(c) Load Dipping: This research has revealed additional transient load dips in the force-displacement curves, well beyond the knee point, with their Frequency found to be dependent on the indenter size. Out of all the indenters, the 4 mm indenter shows the maximum number of load dips. These dips correspond to the failure of a fiber bundle or a group of fibers, with a larger indenter engaging more fibers and thus producing more frequent failure events. After this initial

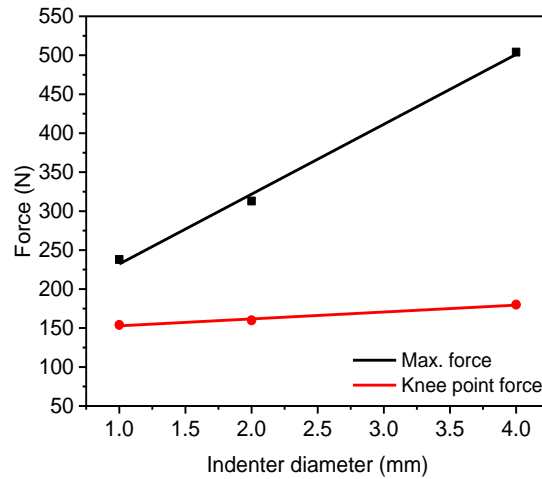


Fig. 5 Influence of indenter diameter on effective force response during quasi-static loading

load dip, there is enough additional load transferred from broken fibers to subsequent fibers to produce an increase in load. The first transient load dip observable in the quasi-static tests indicates audible fiber breakage. Based on results for the 4 mm indenter, the 1st load dip occurs at 452 N (final failure at 504 N), implying the laminate carries an additional 52 N of load after initial fiber failure. The load dip associated with this further cyclic deformation can only be very modest for a 2 mm indenter (303 N with final failure at 313 N) (i.e., an additional 10 N load after initial yield).

In contrast, for the 1 mm indenter, a meaningful, well-defined load dip is no longer observed. The first fiber breakage corresponds effectively to the final failure load, resulting in instantaneous penetration as the number of fibers involved is extremely limited when the smaller indenter is adopted. These findings have significant implications for materials testing and composite materials design.

(d) End of loading (Final failure): The load that can no longer be supported is called the final failure of the laminate, which is termed the penetration of the material by the indenter. In this stage, a steep decrease in the force-displacement curve indicates a critical damage has occurred. The ultimate failure load depends on the size of the indenter, as larger indenters tend to have larger failure loads related more to the broader distribution of contact stresses, but, importantly, the immediate penetration of the 1 mm indenter shows how localized the damage is for smaller indenters.

(e) Maximum Force: The steep decrease in load after the maximum force indicates final failure. The maximum compaction force reduces with decreasing indenter diameter: 500N for the 4 mm indenter, 350N for the 2 mm indenter, and ~250N for the 1 mm indenter. This decrease is owing to the reduction of the contact area of the indenter and the specimen with the decline of the indenter size. With narrower and sharper indenters, a greater penetration of the laminate, where some of the applied work is used to create penetration energy and fiber breakage damage on top of bending energy, and any additional damage energy. This is unlike the effect of larger diameter indenters, for which the vast majority of the proposed work is used for energy in bending and damage. Penetration effects become negligible. This difference is mainly attributed to the effect of indenter

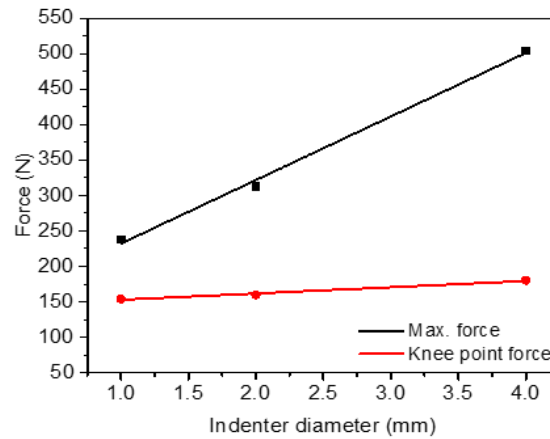


Fig. 6 Representative delamination patterns observed in the composite layups

size, and plays a crucial role in CFRP laminates' behavior during quasi-static loading as well as energy distribution between the failure mechanisms.

The effect of an indenter diameter on the maximum support force of CFRP laminates until failure appears in Figure 5. The force on failures exhibits clear dependence on indenter size (1 mm, 2 mm, 4 mm). The knee point loads, however, are nearly the same for all diameters, suggesting that bending stresses can drive delamination initiation, not indenter size.

The relationship between indenter size and the maximum force and knee point load curves is approximately linear. Despite the effective surface area created during contact, the insignificant differences in indentation behaviour underline the conclusion that the knee point load at which delamination initiation occurs is primarily dictated by bending stresses in lower plies as opposed to indenter size. In contrast, a direct dependence of the peak force on the indenter diameter is shown, where final failure occurs due to fiber breakage beneath the indenter, such that larger indenters distribute contact stresses over a larger area, ultimately affecting the resistance against loading. This difference indicates that the size of the indenter is an important parameter affecting the transition from delamination initiation to complete failure of laminated composites.

5.2 Internal damage

In order to evaluate the shapes and characteristics of damage, a specimen was taken from the impacted area of the damaged carbon fiber reinforced polymer (CFRP) laminate for three-dimensional (3D) scanning. The first step was to cut the damaged specimen into smaller pieces to examine the damage morphology under a microscope. The sample was polished and ground to a quality suitable for high-resolution imaging before it was subjected to microscopic analysis. This pretreatment procedure is, nevertheless, known not to provide a complete description of the damage within the laminate, i.e., fiber breakage, matrix cracking, and delamination. Additionally, the cutting process itself might cause further damage because, to cut the appropriate area, the damaged area must be cut through. Characterization of the delamination morphology at the cut sample edge is shown in Fig. 6, indicating an initial representation of the kind of damage profiles present in the affected zone.

The current investigation carefully identified and visualized the delamination areas and matrix

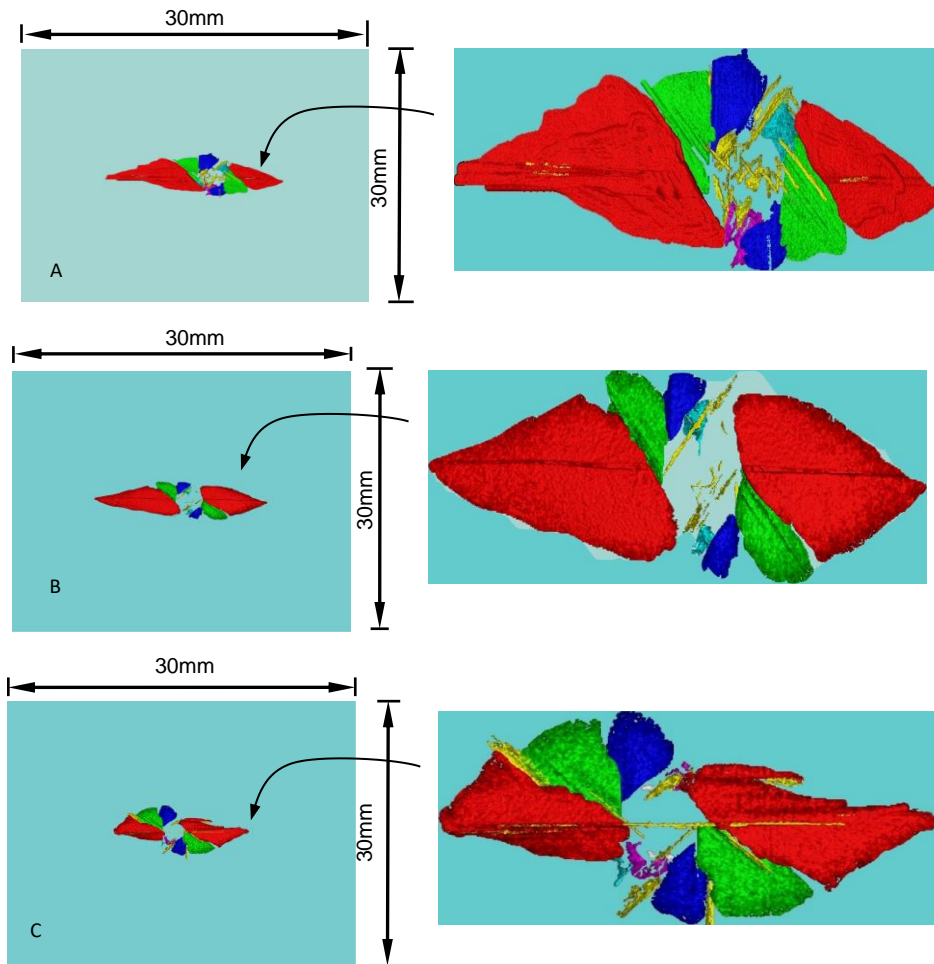


Fig. 7 Delamination zones between adjacent laminate plies under quasi-static loading, captured via CT scanning for various indenter diameters: (A) 4 mm, (B) 2 mm, and (C) 1 mm

cracking in the carbon fiber reinforced polymer (CFRP) laminate. Using VG Studio software, individual colours were assigned to different types of damage and different delamination layers through the various plies. It was documented that the delaminated region was moving forward toward the back face of the laminate, which is the tension side. The delaminated area characteristics, such as size and shape, depend on various factors, including the layup of nearby plies, laminate thickness, mechanical properties of the cohesive interface, and indenter geometry.

As shown in Fig. 7, the delamination area increases with the Indenter diameter (1mm, 2mm & 4mm). The explanation for this trend lies in differences in the stresses generated by indenters of various sizes, it is mentioned that smaller-radius indenters create localized high stresses, encouraging localized matrix failure with fiber breakage, while larger-radius indenters yield modes more focused on global elastic deformation, which is later relieved by delamination. While the size of the delamination area varied, the delamination shape for the three indenter sizes remained consistent, with the shape of the delamination primarily determined by the fiber

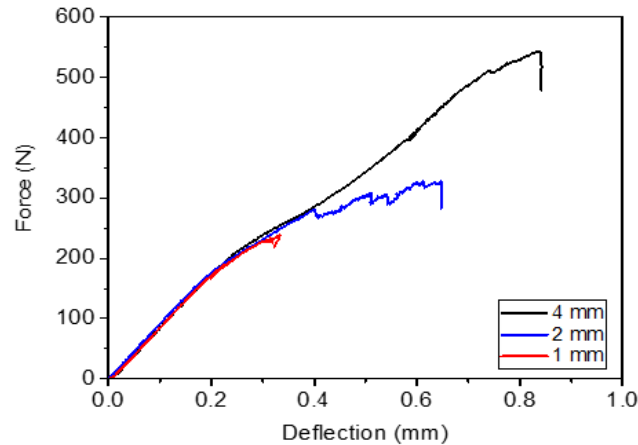


Fig. 8 Force-displacement curve of three indenters

orientation in the adjacent plies. In this study, the angular difference between adjacent plies is 45° , as defined by the laminate stacking sequence $[0, 45, 90, -45]_s$. Therefore, variations in the size of the delamination area were mainly based on the position of the ply concerning the impact point, rather than based on differences in inter-ply angles.

To confirm the results of the experiment, the force-displacement curves for the 1 mm, 2 mm, and 4 mm indenter diameters were generated in the simulation stage of this study using the finite element software ABAQUS. Fig. 8 shows such simulated curves that can serve as an illustration to be a legitimate comparison way of evaluation, checking whether the numerical model is forming similar force response and displacement profiles to the quasi-static behavior of the CFRP (carbon fiber reinforced polymer) laminates for different indenter sizes.

The force-displacement curves obtained from the ABAQUS simulations shown in Figure 8 closely reflect the experimental results for carbon fiber reinforced polymer (CFRP) laminates under quasi-static loading with three indenter diameters (1 mm, 2 mm, 4 mm). Four specific details stand out here that highlight how well the model captures the mechanical response and damage evolution:

(a) *Elastic Region*: The beginning linear sections of the curves display a parallel slope for all the indenter sizes, signifying elastic deformation. This agreement confirms the performance of the ABAQUS model in the laminates' elastic stiffness modeling before the damage initiation, where the laminate behavior is relatively accurate.

(b) *Knee Point*: All three curves have shown one significant knee point corresponding to 0.2 mm displacement, indicating a change of slope due to the onset of delamination. Indenter size is shown not to affect the slope after the knee point, therefore suggesting that in this regime the means of failure is dominated by delamination. The model accurately represents the observed decrease in laminate stiffness, demonstrating its ability to model this critical transition in structural behavior. (c) *Load Dips*: The ability to observe load dips corresponding to localized failure events, such as fiber bundle fractures, also increases with increasing indenter and matches qualitative experimental observations. Load dip values are reported as 222 N for the 1 mm indenter, 280 N for the 2 mm indenter, and 508 N for the 4 mm indenter. This trend is consistent with the increased engagement of fibers via larger indenters, resulting in more damage events, which the ABAQUS model replicates well.

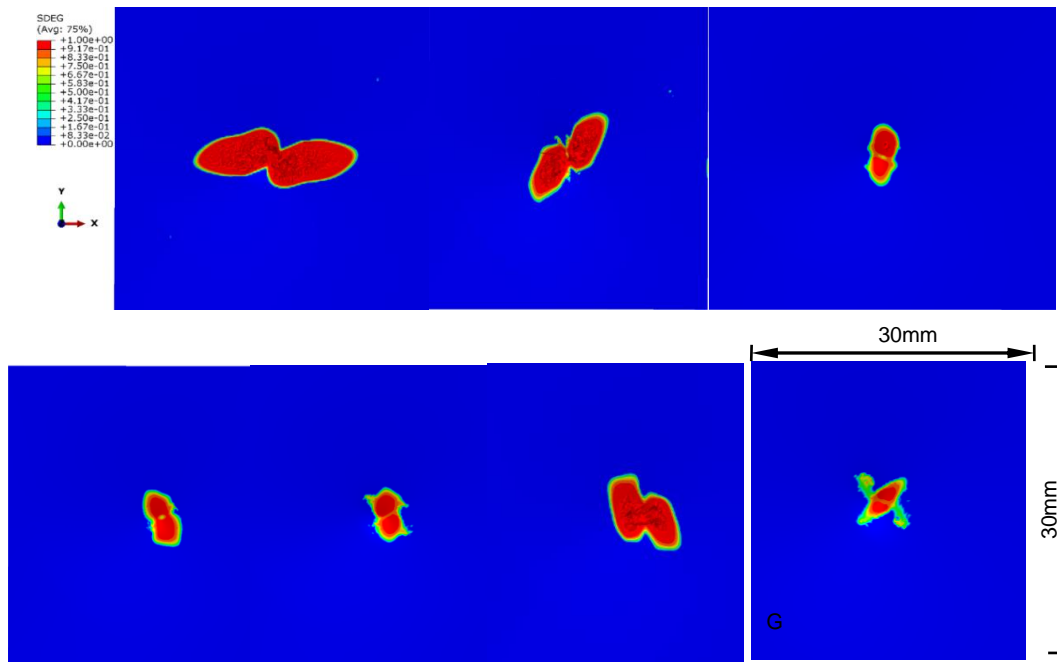


Fig. 9 Delamination areas between different adjacent plies of the laminate subjected to quasi-static loading with a 4 mm impactor: (A) between the 7th and 8th plies, (B) between the 6th and 7th plies, (C) between the 5th and 6th plies, (D) between the 4th and 5th plies, (E) between the 3rd, 4th, and 5th plies, (F) between the 2nd and 3rd plies, and (G) between the 1st and 2nd plies.

(d) *Peak Force*: There is a strong dependence of peak force on indenter size, with peak values of 222 N, 321 N, and 539 N for the 1 mm, 2 mm, and 4 mm indenters, respectively. This peak force reduction with smaller indenters is explained by the higher localized stress concentrations leading to earlier fiber failure. The model's ability to reproduce this size influence demonstrates its strength in predicting total failure under various contact conditions.

The present findings verify the ability of the ABAQUS model to faithfully reproduce the elastic response, delamination initiation, localized failure mechanisms, and ultimate load capacity of CFRP laminates. Such close agreement with experimental data bolsters confidence in the model's predictive capabilities, thereby allowing the model to be utilized for the design and analysis of composite structures under quasi-static loading. Both curves show good agreement, indicating the model accurately captures material behavior up to failure. Slight deviation near peak force suggests possible differences in damage initiation or boundary conditions.

A realistic zone model has been adopted to model the delamination morphology between two adjacent plies in the carbon fiber reinforced polymer (CFRP) laminate. The cohesive layer's thickness (1×10^{-6} m) was set to represent the actual surface and the interlaminar damage growth accurately. In this study, delamination was modeled using the Quadratic Stress (QUADS) criterion, which has been shown to outperform the maximum nominal stress criterion. This increased accuracy is due to the QUADS criterion's consideration of interactions between normal and shear components of stress in two directions, as opposed to the maximum nominal stress method, which neglects these correlations. The employed modeling strategy allows for a more accurate prediction of delamination initiation and propagation of damage, improving the overall understanding of damage evolution within composite structures.

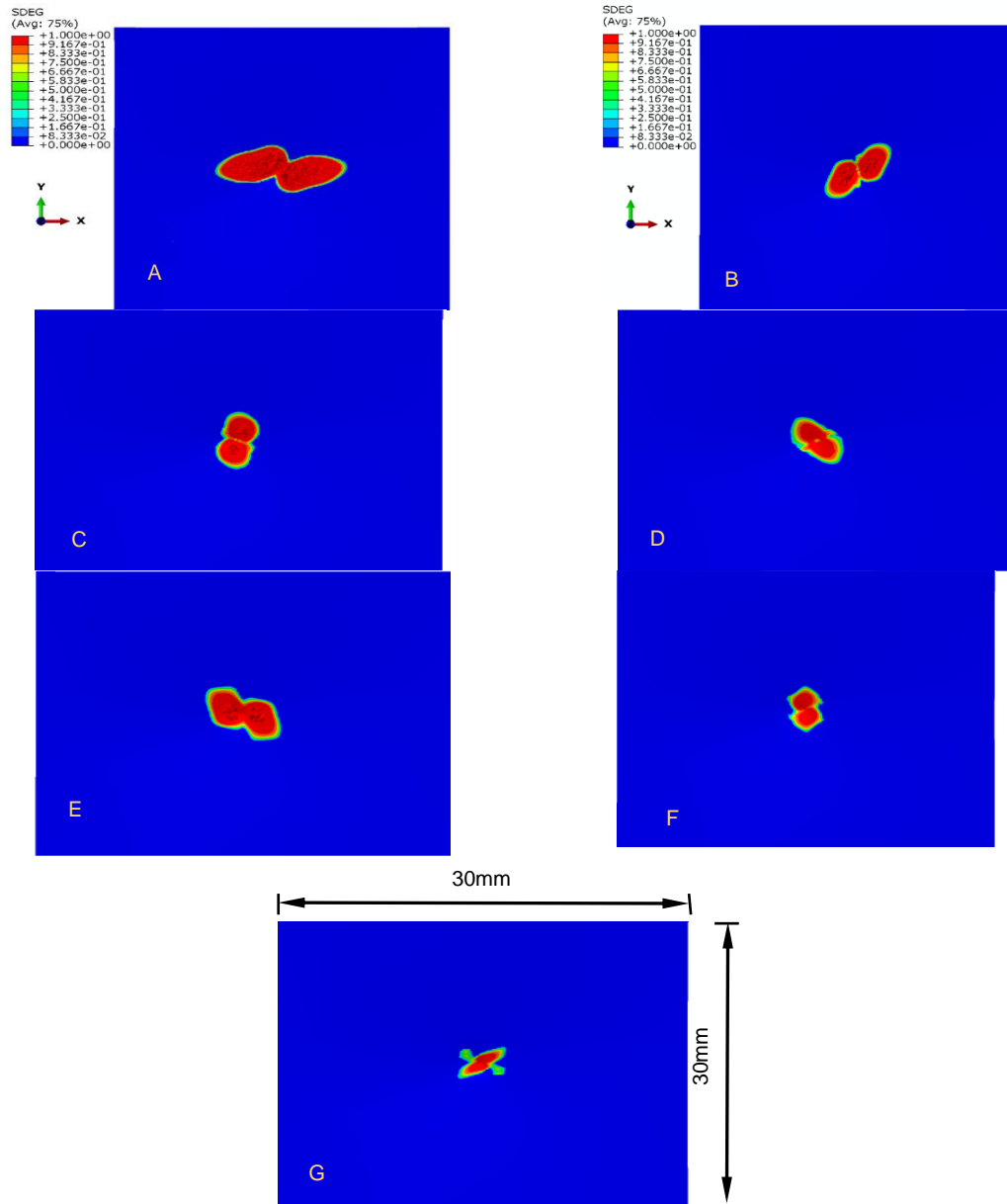


Fig. 10 Delamination zones between various adjacent plies of the laminate subjected to quasi-static loading using a 2 mm impactor. (A) Separation between the 7th and 8th plies. (B) Between the 6th and 7th plies. (C) Between the 5th and 6th plies. (D) Between the 4th and 5th plies. (E) Between the 3rd and 4th plies. (F) Between the 2nd and 3rd plies. (G) Between the 1st and 2nd plies

As illustrated by the damage morphology presented in Figures 9 to 12, for the same impact energy, the fiber directions of the adjacent plies play a vital role in the damage progression. The shape of the delamination is always in the Form of an eight shape, with the central axis of the eight coinciding with the bottom ply fiber orientation and the minor axis oriented with the fiber

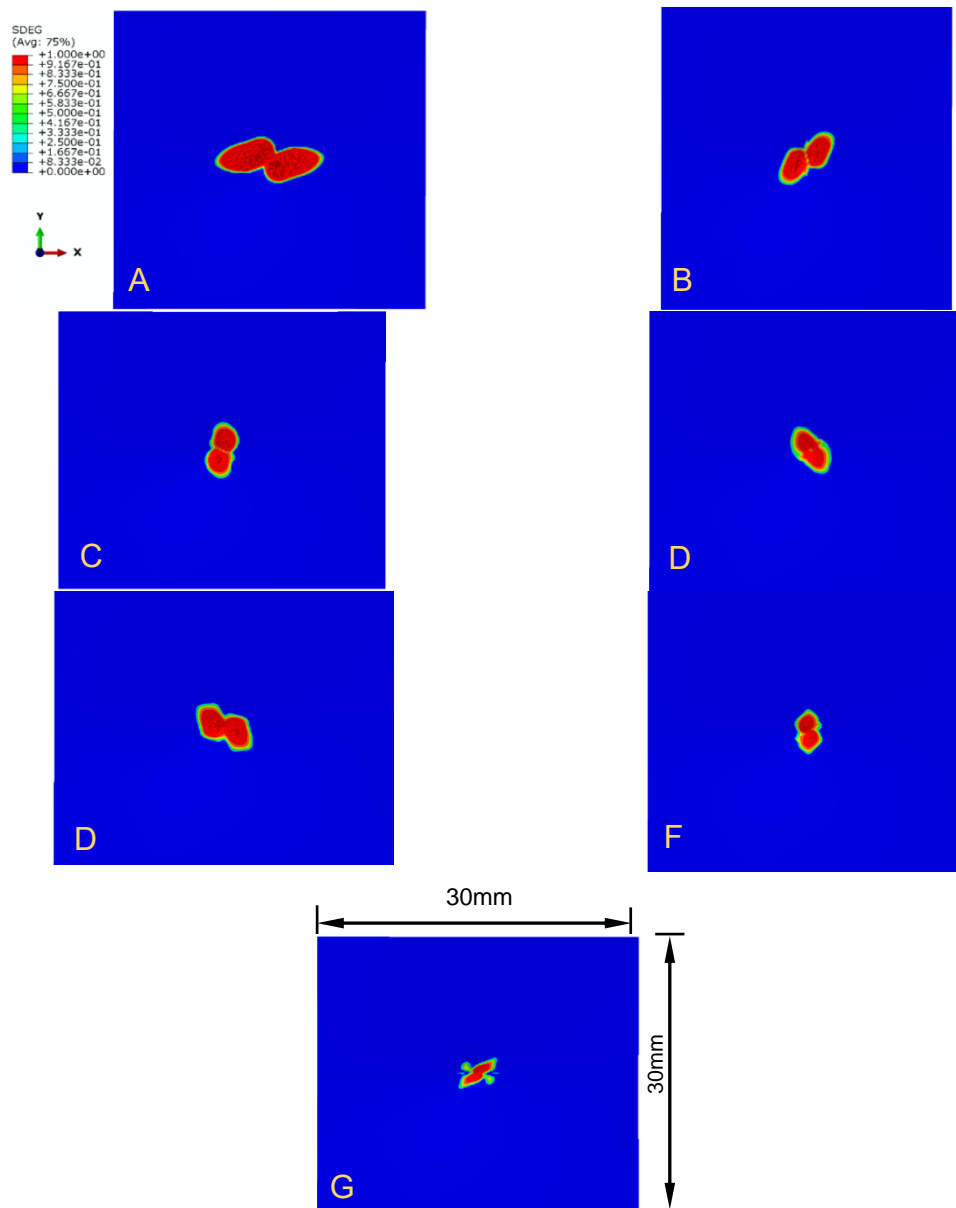


Fig. 11 Delamination regions observed between successive laminate plies under quasi-static loading using a 2 mm diameter impactor: (A) between the 7th and 8th plies, (B) 6th and 7th, (C) 5th and 6th, (D) 4th and 5th, (E) 3rd and 4th, (F) 2nd and 3rd, and (G) 1st and 2nd plies

direction of the top ply. The size and shape of the delaminated region are determined not only by the distortion pattern but also by other factors such as proximity to the impact point, where the region might experience tensile or compressive stresses. Shear stress or tensile stress is mainly responsible for the delamination. Delamination at the laminate mid-thickness region primarily occurs as a result of shear stress, whereas the dominant delamination farther away from the point

of impact occurs due to tensile stresses caused by bending. As the compressive loading increases, these tensile stresses lead to matrix cracking within the affected area. Some cracks, aligned in a vertical direction as a result of tensile bending, extend to the interface between neighboring plies, which a) triggers or b) advances delamination in these areas. Overall, this interrelationship of applied states of stress and propagation mechanisms of cracking reflects the damage response in terms of laminate structural response to quasi-static loads.

5.3 Comparison between experimental results and numerical modelling outcomes

To validate the numerical simulations, the force-displacement curves obtained from the numerical simulations are plotted against the experimental curves for the three indenter diameters (1 mm, 2 mm, and 4 mm). The direct comparison with experimental results allows cross-checking of results and ensures the simulation is capturing the quasi-static response of carbon-fiber-reinforced polymer (CFRP) laminates.

As the force-displacement curves in Figs (12, 13 and 14) illustrate, the global responses of damaged carbon fiber reinforced polymer (CFRP) laminates under quasi-static loading for different indenter diameters (1 mm, 2 mm, and 4 mm) are highly similar. This similarity, with the experimental and numerical results matching closely, instills confidence in the accuracy of our research. Using ABAQUS for numerical modeling, all essential features from the experimental force-displacement curves, such as knee loads and load dips, are well captured for all the test cases. The four distinct features identified in Figure 4 were replicated in the simulated results with varying degrees of fidelity as described below:

(a) *Elastic Region:* The elastic region of both experimental and simulated responses for all three indenter sizes appears to be consistent. The slopes of the force-displacement curves in this region are nearly matched exactly here also, as expected, due to the modeling being performed to match the experimental boundary and initial conditions, accurately reflecting the laminate's elastic stiffness.

(b) *Knee Point:* The proposed knee point, around 0.2 mm displacement, is captured accurately, matching experimental data closely. From the knee point onwards, the slope of the force-displacement contributes remains identical for all experimental and simulation results which suggests that the model is also capable of simulating the onset of delamination and the loss of stiffness of the laminate.

(c) *Load Dips:* Load dips in the simulated results also show trends similar to experimental observations, in terms of an increase in the dip frequency with increasing indenter size. For the 1 mm, 2 mm, and 4 mm indenters, the load dip values for the experimental tests were 239 N, 303 N, and 508 N, the load dip values for the simulations were 239 N, 273 N, and 508 N. This close match highlights the model's capability to reproduce localized failure events, such as how fiber bundles break.

(d) *Peak Force:* All three indenter sizes exhibit a slight difference in peak force between the experimental results and simulation data. The peak forces for the 4 mm indenter are 504 N (experimental) and 538 N (simulated), for the 2 mm indenter, 313 N (experimental) and 324 N (simulated), and for the 1 mm indenter, 239 N (experimental) and 232 N (simulated). While there are minor differences between these datasets, this is expected given the complex nature of capturing final failure mechanisms, however, the overall trend of increasing peak force with increasing indenter diameter is consistently observed.

All the aforementioned results validate the performance of the ABAQUS model in predicting

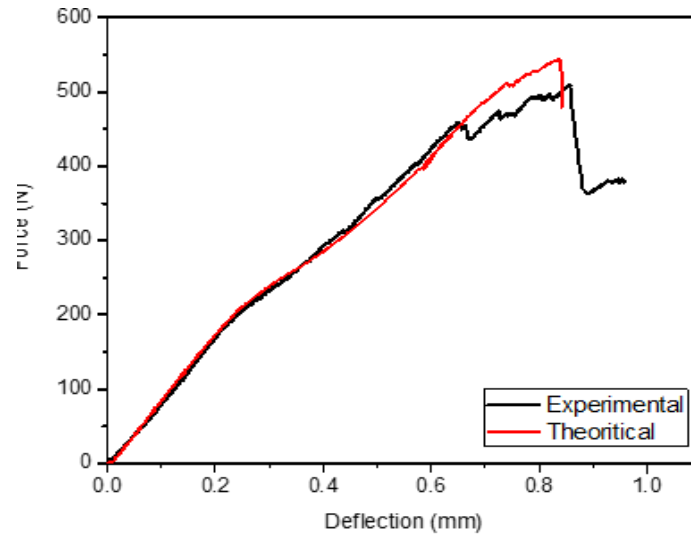


Fig. 12 Force-displacement curve of 4mm diameter

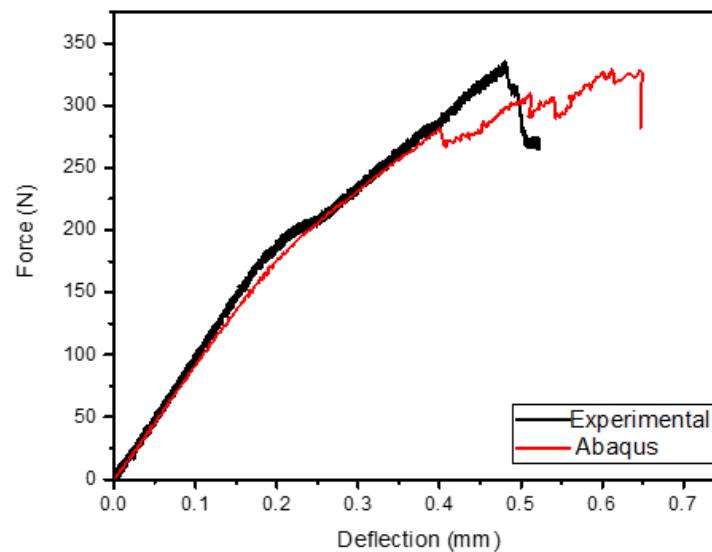


Fig. 13 Force-displacement curve of 2mm diameter

the elastic response, delamination initiation, localized failure events, and peak load behaviour of such CFRP laminates under quasi-static loading. The plot shows a strong correlation between experimental and Abaqus simulation results for force versus displacement, confirming the simulation's validity in capturing the structural response. The force increases nonlinearly with displacement, showing material hardening followed by a peak and slight softening, indicating the onset of damage or failure. Minor discrepancies near the peak load may be due to simplifications in the finite element model, such as idealized boundary conditions, material assumptions, or strain rate effects not captured in the simulation.

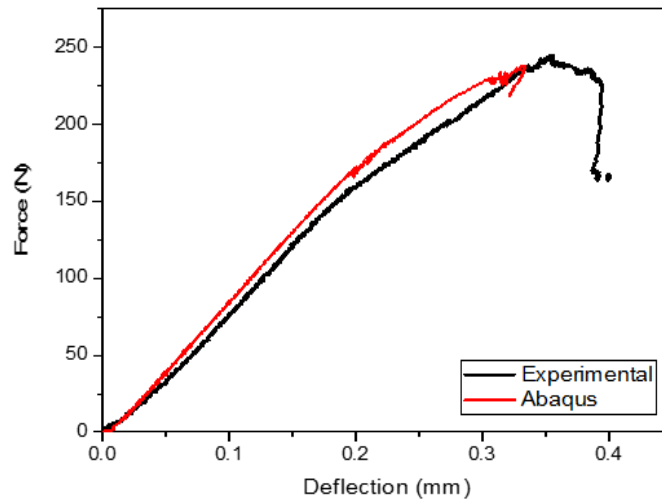


Fig. 14 Force-displacement curve of 1mm diameter

6. Conclusions

This study concluded that CFRP structures are susceptible to matrix cracks, delamination, and fiber breakage under quasistatic and low-velocity impact loading. It is one of the primary mechanisms for absorbing energy, especially at low speeds, when delamination occurs. Loading rate influences CFRP laminate mechanical response. It is more damaging to the internal structure from impact loading than quasistatic loading when energy levels are similar. It is essential to consider the stacking sequence and ply orientation when considering impact resistance and energy absorption capability. Moreover, the dispersion of impact energy is often better with cross-ply or quasi-isotropic laminates.

There is a significant reduction in residual compressive or tensile strength following quasistatic indentation as well as impact damage. However, the study is limited by some limitations, including the use of drop-weight testers to simulate idealized low-velocity impacts, which are not fully representative of real-world events generally limited to specific CFRP types, matrix systems, or layups - thus, not generalizable.

The indenter size plays a vital role in the type of damage, i.e., penetration or delamination. Also, the simulation work has the potential to predict the damage size and shape.

Some studies rely on surface observations or basic ultrasonic techniques, missing finer internal damage like matrix microcracks. Temperature, humidity, and aging effects are often ignored, even though they significantly influence composite behavior. Future Research Directions employ studying hybrid CFRP laminates (e.g., CFRP/GFRP or CFRP/metal hybrids) to enhance toughness and impact resistance, and embedding sensors or self-healing capabilities to monitor and mitigate damage progression. The potential future research direction is to examine significant components to define the accurate location of the damage to avoid the catastrophic damage of the composite structure, and further work is needed to explore the microcracks at low load impacts. However, the limitation of this technique is that it requires a large CT scan. Delamination due to hidden internal layer separations can also seriously compromise structural integrity without affecting surface appearance. The resin matrix is also brittle, which compromises load transfer between fibers when damaged.

References

- Abbas, E.N., Abud Ali, Z.A.A., Njim, E.K., Flayyih, M.A. and Madan, R. (2025), "Analytical and numerical investigation of free vibration of nanoparticle-reinforced composite cylindrical shells", *Diagnostyka*, **26**(1), 1-12. <https://doi.org/10.29354/diag/201249>
- Akbulut, M., Sarac, A. and Ertas, A.H. (2020), "An investigation of non-linear optimization methods on composite structures under vibration and buckling loads", *Adv. Comput. Des.*, **5**(3), 209-231. <https://doi.org/10.12989/ACD.2020.5.3.209>
- Ali, A.Y. and Hasan, H.M. (2022), "Non-linear large amplitude vibration of orthotropic FGM convex and concave toroidal shell segments including the damping effect using the shear deformation theory", *Thin Wall. Struct.*, **173**, 109035. <https://doi.org/10.1016/j.tws.2022.109035>
- Alhous, Z.F.A., Jweeg, M.J., Njim, E.K., Mouthanna, A., Flayyih, M.A., Madan, R., Khobragade, P. and Rai, P.K. (2025), "Nonlinear frequency and dynamic response of PLA polymeric imperfect FG sandwich plates under hygrothermal conditions", *Coupled Syst. Mech.*, **14**(1), 1-19. <https://doi.org/10.12989/CSM.2025.14.1.001>
- Azeez Neamah, R., Ahmed Nassar, A., Alansari, L.S., Kadum Njim, E., Hadji, L. and Madan, R. (2025), "Static deflection analysis of functionally graded beams using various beam theories", *Math. Modell. Numer. Simul. Appl.*, **5**(2), 396-420. <https://doi.org/10.53391/mmnsa.1524642>
- Hassan, A., Jadoo, A., Bakhy, S., Njim, E. and Al-Maliky, F. (2025), "Analysis of Electric Vehicle (EV) transmission performance through helical rotor gear systems with variable Helix angles", *ASEAN J. Sci. Eng.*, **5**(2), 357-368. <https://doi.org/10.17509/ajse.v5i2.87802>
- Başoğlu, F., Yakar, E.C., Bora, M. Ö. and Tuna, V. (2023), "Comparison of low-velocity impact behavior of thick laminated composite structure with experimental and modeling technique", *Polym. Compos.*, **44**(11), 7657-7673. <https://doi.org/10.1002/pc.27654>
- Brethee, K.F., Uwayed, A.N. and Alden Qwam, A.Y. (2023), "A novel index for vibration-based damage detection technique in laminated composite plates under forced vibrations: experimental study", *Struct. Health Monitor.*, **22**(5), 3109-3125. <https://doi.org/10.1177/14759217221145622>
- Daneshmand, S., Vini, M.H., Sajadi, S.M., Mouthanna, A., Jasim, D.J., Hammoodi, K.A., Hekmatifar, M. and Navid Nasajpour-Esfahani (2023), "Numerical and experimental investigations of mechanical, tribological, and electrical properties of laminated Bi-metal Al/SiC/Ni composites", *Mater. Today Commun.*, **37**, 107355. <https://doi.org/10.1016/j.mtcomm.2023.107355>
- Davies, G.A.O. and Zhang, X. (1995), "Impact damage prediction in carbon composite structures", *Int. J. Impact Eng.*, **16**(1), 149-170. [https://doi.org/10.1016/0734-743X\(94\)00039-Y](https://doi.org/10.1016/0734-743X(94)00039-Y)
- Falzon, B.G. and Apruzzese, P. (2011), "Numerical analysis of intralaminar failure mechanisms in composite structures. Part I: FE implementation", *Compos. Struct.*, **93**(2), 1039-1046. <https://doi.org/10.1016/j.compstruct.2010.06.028>
- Fayyadh, M.M. (2021), "Modified models to predict the ultimate flexural and shear capacities of CFRP repaired RC beams", *Adv. Comput. Des.*, **6**(2), 99-115. <https://doi.org/10.12989/ACD.2021.6.2.099>
- Ibrahim, G.R., Albarbar, A. and Brethee, K.F. (2021), "Progressive failure mechanism of laminated composites under fatigue loading", *J. Compos. Mater.*, **55**(1), 137-144. <https://doi.org/10.1177/0021998320944990>
- Johnson, A.F. and Holzapfel, M. (2006), "Influence of delamination on impact damage in composite structures", *Adv. Statics Dyn. Delaminat.*, **66**(6), 807-815. <https://doi.org/10.1016/j.compstruct.2004.12.032>
- Kadum Njim, E., Al-Maamori, M.H., Madan, R., Bakhy, S.H., Al-Waily, M., Khobragade, P. and Hadji, L. (2025), "Numerical and analytical investigation of free vibration behavior of porous functionally graded sandwich plates", *Mech. Adv. Compos. Struct.*, **12**(3), 555-568. <https://doi.org/10.22075/macs.2024.34962.1710>
- Khudhur, R.I.M., Njim, E.K., Jweeg, M.J., Al-Waily, M., Hameed, A.A. and Jamil, A. (2025), "Numerical simulation for the vibration of rotating leaf springs used in the cement kiln of the cement plant: A

- computerized analysis”, *IET Conference Proceedings*, **2024**(34), 28-33.
<https://doi.org/10.1049/icp.2025.0056>
- Kobayashi, A.S., Chiu, S.T. and Beeuwkes, R. (1973), “A numerical and experimental investigation on the use of J-integral”, *Eng. Fract. Mech.*, **5**(2), 293-305. [https://doi.org/10.1016/0013-7944\(73\)90024-6](https://doi.org/10.1016/0013-7944(73)90024-6)
- Liu, P.F. and Zheng, J.Y. (2010), “Recent developments on damage modeling and finite element analysis for composite laminates: A review”, *Mater. Des.*, **31**(8), 3825-3834.
<https://doi.org/10.1016/j.matdes.2010.03.031>
- LLorca, J., González, C., Molina-Aldareguía, J.M. and López, C.S. (2013), “Multiscale modeling of composites: toward virtual testing ... and beyond”, *JOM*, **65**(2), 215-225.
<https://doi.org/10.1007/s11837-012-0509-8>
- Lin, W. and Wang, Y. (2023), “Low velocity impact behavior of auxetic CFRP composite laminates with in-plane negative Poisson’s ratio”, *J. Compos. Mater.*, **57**(12), 2029-2049.
- Lan, K., Wang, H. and Wang, C. (2023), “Delamination behavior of CFRP laminated plates under the combination of tensile preloading and impact loading”, *Materials*, **16**(19).
<https://doi.org/10.3390/ma16196595>
- Marir, B.S. and Uwayed, A.N. (2024), “Fiber breakage detection using static deflection in laminated composite structures”, *AIP Conference Proceedings*, **3009**(1), 030018. <https://doi.org/10.1063/5.0190418>
- Mohammad, A.H., Al-Waily, M., Njim, E.K., Jweeg, M.J. and Hameed, A.A. (2024), “Design and analysis of artificial IVD by 3D printing technology using functionally graded materials”, *In Lecture Notes in Networks and Systems*, 81-95. Springer Nature Switzerland. https://doi.org/10.1007/978-3-031-70924-1_7
- Mouthanna, A., Hasan, H.M. and Najim, K.B. (2018), “Nonlinear vibration analysis of functionally graded imperfection of cylindrical panels reinforced with different types of stiffeners”, *In Proceedings of the 2018 11th International Conference on Developments in eSystems Engineering (DeSE)*, 284-289, IEEE.
<https://doi.org/10.1109/dese.2018.00057>
- Madan, R., Khobragade, P., Mussada, E.K., Singh, M.K., Rangappa, S.M., Njim, E.K. and Siengchin, S. (2025), “A novel two-step finite element approach to estimate the thermo-mechanical properties of two-phase and three-phase hybrid composites”, *Compos. Commun.*, **53**, 102213.
<https://doi.org/10.1016/j.coco.2024.102213>
- Narwariya, M., Choudhury, A. and Sharma, A.K. (2018), “Harmonic analysis of moderately thick symmetric cross-ply laminated composite plate using FEM”, *Adv. Comput. Des.*, **3**(2), 113-132.
<https://doi.org/10.12989/ACD.2018.3.2.113>
- Nezhad, H.Y., Merwick, F., Frizzell, R.M. and McCarthy, C.T. (2014), “Numerical analysis of low-velocity rigid-body impact response of composite panels”, *Int. J. Crashworth.*, **20**(1), 27-43.
<https://doi.org/10.1080/13588265.2014.963378>
- Nguyen, M.H. and Waas, A.M. (2020), “A novel mode-dependent and probabilistic semi-discrete damage model for progressive failure analysis of composite laminates - Part I: Meshing strategy and mixed-mode law”, *Compos. Part C*, **3**, 100073. <https://doi.org/10.1016/j.jcomc.2020.100073>
- Nolan, R.L. (2012), “Ubiquitous IT: The case of the Boeing 787 and implications for strategic IT research”, *20th Anniversary Special Issue*, **21**(2), 91-102. <https://doi.org/10.1016/j.jsis.2011.12.003>
- Olsson, R., Donadon, M.V. and Falzon, B.G. (2006), “Delamination threshold load for dynamic impact on plates”, *Int. J. Solids Struct.*, **43**(10), 3124-3141. <https://doi.org/10.1016/j.ijsolstr.2005.05.005>
- Perillo, P.G. and Jørgensen, J.K. (2016), “Numerical/experimental study of the impact and compression after impact on GFRP composite for wind/marine applications”, *Procedia Eng.*, **167**, 129-137.
<https://doi.org/10.1016/j.proeng.2016.11.679>
- Panigrahi, S.K. and Das, K. (2016), “Ballistic impact analyses of triangular corrugated plates filled with foam core”, *Adv. Comput. Des.*, **1**(2), 139-154. <https://doi.org/10.12989/ACD.2016.1.2.139>
- Phocas, M.C., Georgiou, N. and Christoforou, E.G. (2022), “A class of actuated deployable and reconfigurable multilink structures”, *Adv. Comput. Des.*, **7**(3), 189-210.
<https://doi.org/10.12989/ACD.2022.7.3.189>
- Polatov, A.M., Khaldjigitov, A.A. and Ikramov, A.M. (2020), “Algorithm of solving the problem of small elastoplastic deformation of fiber composites by FEM”, *Adv. Comput. Des.*, **5**(3), 305-321.

- <https://doi.org/10.12989/ACD.2020.5.3.305>
- Raad, H., Najim, E.K., Jweeg, M.J., Al-Waily, M., Hadji, L. and Madan, R. (2024), "Vibration analysis of sandwich plates with hybrid composite cores combining porous polymer and foam structures", *J. Comput. Appl. Mech.*, **55**(3), 485-499. <https://doi.org/10.22059/jcamech.2024.377658.1121>
- Schoeppner, G.A. and Abrate, S. (2000), "Delamination threshold loads for low velocity impact on composite laminates", *Compos. Part A Appl. Sci. Manuf.*, **31**(9), 903-915. [https://doi.org/10.1016/S1359-835X\(00\)00061-0](https://doi.org/10.1016/S1359-835X(00)00061-0)
- Sindu, B.S., Alex, A. and Sasmal, S. (2018), "Studies on structural interaction and performance of cement composite using Molecular Dynamics", *Adv. Comput. Des.*, **3**(2), 147-163. <https://doi.org/10.12989/ACD.2018.3.2.147>
- Song, K., Dávila, C.G., and Rose, C.A. (2008), "Guidelines and parameter selection for the simulation of progressive delamination", *Proceedings of the 2008 Abaqus Users' Conference*. <https://ntrs.nasa.gov/citations/20080020385>
- Tabiei, A. and Zhang, W. (2018), "Composite laminate delamination simulation and experiment: A review of recent development", *Appl. Mech. Rev.*, **70**(030801). <https://doi.org/10.1115/1.4040448>
- Uwayed, A.N. and Abbood, M.Y. (2022), "Analytical and theoretical study of vibration-based damage detection technique in a composite structure", *Int. J. Comput. Aid. Eng. Technol.*, **17**(1), 23. <https://doi.org/10.1504/IJCAET.2022.124527>
- Uwayed, A.N., Brethee, K.F. and Muhammad, S.O. (2023), "Improved vibration based damage detection in laminated composite plate structures under free and forced modal analysis", *Eur. J. Mech. A Solids*, **100**, 105031. <https://doi.org/10.1016/j.euromechsol.2023.105031>
- Vini, M.H. and Daneshmand, S. (2022), "Mechanical and wear properties evaluation of Al/Al₂O₃ composites fabricated by combined compo-casting and WARB process", *Adv. Comput. Des.*, **7**(2), 129-137. <https://doi.org/10.12989/ACD.2022.7.2.129>
- Wimmer, G., Schuecker, C. and Pettermann, H.E. (2009), "Numerical simulation of delamination in laminated composite components - A combination of a strength criterion and fracture mechanics", *Compos. Part B Eng.*, **40**(2), 158-165. <https://doi.org/10.1016/j.compositesb.2008.10.006>
- Xiao, L., Lu, C., Li, X., Xu, N., Zheng, T., Wang, G., Wang, X. and Zhang, D. (2023), "Exploration of impact response and damage mechanism of discontinuous CFRP laminates subjected to low velocity impact", *Polym. Compos.*, **44**(11), 7657-7673. <https://doi.org/10.1002/pc.27654>
- Xiao, L., Lu, C., Li, X., Xu, N., Zheng, T., Wang, G. and Zhang, D. (2023), "Exploration of impact response and damage mechanism of discontinuous CFRP laminates subjected to low velocity impact", *Polym. Compos.*, **44**(10), 6324-6336. <https://doi.org/10.1002/pc.27561>
- Zhang, X. (1998), "Impact damage in composite aircraft structures-experimental testing and numerical simulation", *Proceedings of the Institution of Mechanical Engineers, Part G: Journal of Aerospace Engineering*, **212**(4), 245-259. <https://doi.org/10.1243/0954410981532414>
- Zhang, X., Bianchi, F. and Liu, H. (2012), "Predicting low-velocity impact damage in composites by a quasi-static load model with cohesive interface elements", *Aeronaut. J.*, **116**(1186), 1367-1381. <https://doi.org/10.1017/S0001924000007685>
- Zhou, J., Wen, P. and Wang, S. (2020), "Numerical investigation on the repeated low-velocity impact behavior of composite laminates", *Compos. Part B Eng.*, **185**, 107771. <https://doi.org/10.1016/j.compositesb.2020.107771>